NIH RELAIS Document Delivery

NIH-10286766

JEFFDUYN

NIH -- W1 MA34IF

JOZEF DUYN
10 Center Dirve
Bldg. 10/Rm.1L07
Bethesda, MD 20892-1150

ATTN:
PHONE: 301-594-7305
FAX: -
E-MAIL:

SUBMITTED: 2002-08-29 17:22:17
PRINTED: 2002-09-03 07:33:11
REQUEST NO.:NIH-10286766
SENT VIA: LOAN DOC
7967420

NIH Fiche to Paper Journal

TITLE:	MAGNETIC RESONANCE IN MEDICINE : OFFICIAL JOURNAL OF THE SOCIETY OF MAGNETIC RESONANCE IN MEDICINE / SOCIETY OF MAGNETIC RESONANCE IN MEDICINE
PUBLISHER/PLACE:	Wiley-Liss, Inc., a division of John Wil New York, NY :
VOLUME/ISSUE/PAGES:	1995 Jan;33(1):101-7 101-7
DATE:	1995
AUTHOR OF ARTICLE:	Duyn JH; Frank JA; Moonen CT
TITLE OF ARTICLE:	Incorporation of lactate measurement in multi-spin
ISSN:	0740-3194
OTHER NOS/LETTERS:	Library reports holding volume or year 8505245 7891522
SOURCE:	PubMed
CALL NUMBER:	W1 MA34IF
REQUESTER INFO:	JEFFDUYN
DELIVERY:	E-mail: jhd@helix.nih.gov
REPLY:	Mail:

NOTES

Incorporation of Lactate Measurement in Multi-Spin-Echo Proton Spectroscopic Imaging

Jeff H. Duyn, Joseph A. Frank, Chrit T.W. Moonen

An improved multi-slice, multi-spin-echo proton spectroscopic imaging method for human brain is presented. The technique allows the reconstruction of lactate images, along with choline plus creatine, *N*-acetylaspartate, and lipid images from one single data set processed in three separate ways. The discrimination between resonances of lipid protons and lactate methyl protons is based on homonuclear spin-spin coupling. The reliability of the separation of the lipid and lactate contribution depends on the T_2 of the lipid resonances. Measurements were performed on a standard 1.5 Tesla clinical scanner on healthy volunteers and a patient with high grade CNS lymphoma, demonstrating the ability to obtain high quality metabolite maps within 11 min.

Key words: MR proton spectroscopy; MR proton spectroscopic imaging; lactate editing; lipid suppression.

INTRODUCTION

Because of its sensitivity as a marker of anaerobic metabolism, the measurement of local lactate concentration has become one of the prime targets of *in vivo* proton NMR spectroscopy. For example, the concentration of lactate in early stroke may change at least an order of magnitude as the direct result of a change from aerobic to anaerobic glucose consumption. In addition, lactate may be found in and around brain tumors because of limited oxygen supply. Other metabolites observed with long echo time proton spectroscopy may provide important additional information, e.g., local *N*-acetylaspartate (NAA) concentration may report on the number of neurons present, choline (Cho) concentration may provide information on the degree of tumor malignancy. Unfortunately, conventional proton spectroscopic imaging (MRSI) typically takes about a half hour for a 1- to 2-ml resolution at 1.5 T. Furthermore, discrimination between lipid and lactate may take additional studies. Recently, it was shown that the duration of a MRSI study can be shortened drastically using multiple spin-echoes. However, the initial technique did not allow the simultaneous measurement of lactate (Lac) along with choline, creatine (Cre), and NAA.

The resonance due to the methyl protons of lactate is a doublet at 1.33 ppm because of the three-bond homonuclear coupling between the single methine proton and the three equivalent methyl protons ($J = 7$ Hz). The major resonances of lipid (triglycerides) can also be found in the same spectral region. Several methods have been developed to specifically select the lactate methyl resonance. Some methods are based on the coupling with the C_α proton using selective decoupling or selective inversion (1–4). Alternatively, editing methods based on zero-quantum (5–9), multiple quantum (7, 9–14), polarization transfer (15–19), and longitudinal spin order (z filter, 20–22) techniques can be employed. In addition, spin-locking pulses can be used to select the lactate doublet (23). However, these methods do not allow simultaneous, full sensitivity, detection of lactate methyl resonances *and* noncoupled resonances of other metabolites with a single acquisition/phase encode step. As a result, multiple data acquisition protocols have been suggested to discriminate lactate and lipid contributions, and to evaluate Cho, Cre, and NAA, as well. Here, we report a modification of the recently introduced fast MRSI method. The method allows simultaneous measurement of Cho+Cre, NAA, and lactate and also allows a limited discrimination between lactate and lipid solely on the basis of different ways of processing. The technique is based on phase modulation of the lactate doublet in subsequent echoes (interval is $1/J$) due to homonuclear coupling, in contrast to the noncoupled resonances which do not show phase modulation. A preliminary account of this work was presented recently (24).

METHODS

Pulse Sequence and *k*-Space Sampling

Measurements were performed on a phantom and on human subjects on a conventional 1.5 T GE/SIGNA scanner (General Electric, Milwaukee, WI) using a standard head coil and standard shielded gradients with 0.01 T/m maximum strength.

The multi-spin-echo proton MRSI method was a modification of the multi-spin-echo method described previously (25). A CHESS pulse sequence was used for water suppression and octagonal outer volume suppression (OVS) for reduction of lipid signals. The use of optimized 180° pulses, and the crusher scheme to avoid unwanted coherences have been explained previously (25). The new multi-spin-echo sequence (Fig. 1) acquired five ech-

MRM 33:101–107 (1995)

From the Laboratory of Diagnostic Radiology Research, Office of Intramural Research, National Institutes of Health (J.H.D., J.A.F.), and National Institutes of Health in Vivo NMR Research Center, Biomedical Instrumentation and Engineering Program, National Center for Research Resources (C.T.W.M.), Bethesda, Maryland.

Address correspondence to: Chrit T.W. Moonen, Ph.D., In Vivo NMR Research Center, BEIP, NCRR, National Institutes of Health, Building 10, room B1D-123, Bethesda, MD 20892.

Received June 21, 1994; revised September 21, 1994; accepted September 23, 1994.

0740-3194/95 $3.00

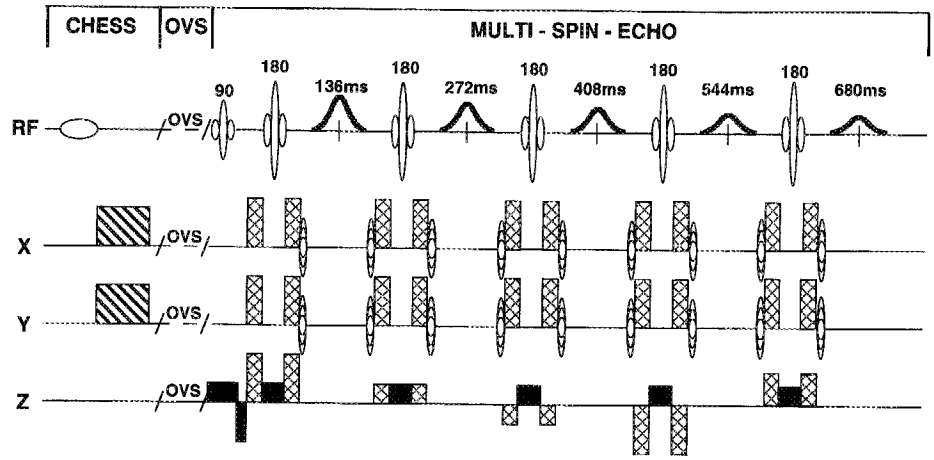

FIG. 1. Multi-spin-echo proton MRSI pulse sequence. CHESS and octagonal OVS are used to suppress water and lipid signals. To allow measurement of lactate, five echoes are generated at intervals of 136 ms. The strength of the z-gradient crusher was varied to suppress stimulated echoes and unwanted gradient echoes.

oes at equidistant intervals of 136 ms (corresponding to $1/J$ for the homonuclear spin-spin coupling of the lactate methyl resonance). The first echo was at 136 ms. An alternative k-space sampling scheme was used in the modified technique (Fig. 2). The central part of k-space was covered by both first and second echo, whereas further segments were covered by later echoes. The double sampling of the central k-space points and the overlap of k-space segments a and b (Fig. 2) is explained below.

The bandwidths of the 90° and 180° RF pulses were 2.0 and 2.2 kHz, respectively. The somewhat larger value for the 180° RF pulse, in combination with equal amplitudes of the slice selection gradients, was chosen to improve the slice profile. This was especially important for the slice profile of the lactate methyl, which was otherwise distorted due to the offset in slice profile of the resonance for the coupled methine proton (26). Experiments on a phantom containing 2 M lactate in water were performed to optimize these slice profiles.

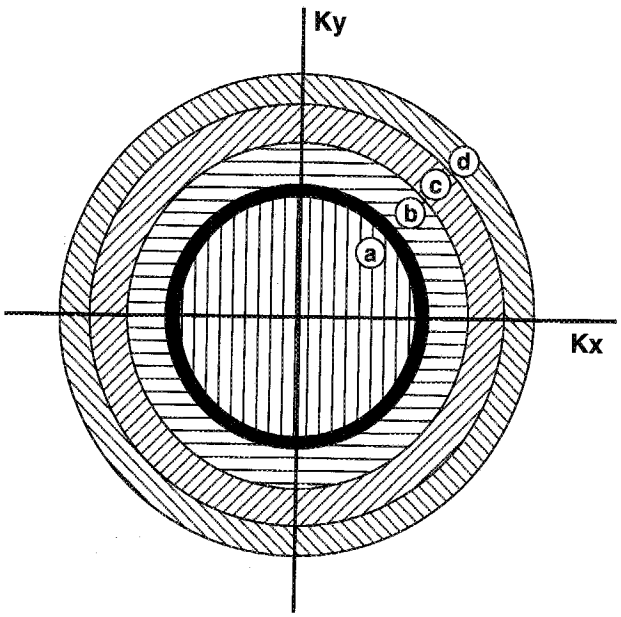

FIG. 2. Segmentation of k-space. The central segment (a) is covered twice, i.e., by the encoding of first and second echo. Further outlying segments (*b,c,d*) are covered by later echoes (3, 4, and 5, respectively). An overlap of segments *a* and *b* (solid black area) was introduced to improve localization of lipid signals.

Data Processing

Data were processed off-line on Sun-SPARC workstations (Sun microsystems, Mountainview, CA) using IDL processing software (Research Systems, Boulder, CO). Each of the five echoes was apodized by a 25% Hamming filter and Fourier transformed. Then, the contribution of the lipid resonances, of the doublet methyl signal of lactate, and of the singlet resonances of the noncoupled resonances of the metabolites Cho, Cre, and NAA were evaluated using three separate ways of processing the same dataset.

Processing method 1 was used to create lipid images. The signals of first and second echo were added, whereas signals of third to fifth echoes were zeroed. In order to null the lactate contribution to the lipid images, a correction for lactate methyl T_2 loss (assuming a T_2 of 1 s) was applied prior to the addition of the first two echoes. The zeroing of the outer k-space segments resulted in a reduction of image resolution to 22 mm.

Processing method 2 was used to create NAA, and Cho+Cre images. The signals from the five echoes were corrected for signal loss due to T_2 decay using a decay constant of 400 ms (25). Subsequently, the signals of first and second echo were added. In the overlapping area of segment *a* and *b* (see Fig. 2, radial overlap = 5 points), a weighted average (Hamming weighting function) was taken of the corresponding signals. This resulted in a smooth apodization of residual lipid signal due to its short T_2. Without this procedure, a step function would be present in the lipid k-space going from segment *a* to *b* due to the short lipid T_2, leading to an increased bleed into neighboring voxels.

Processing method 3 was used to reconstruct lactate images. First, a 180° phase correction was applied to the odd echo signals. Signal losses over subsequent echoes due to T_2 decay were corrected using a 1-s decay constant. Subsequently, signals of echo 1 and 2 were added with relative weighting factors 0.34:1 to null the lipid signal in the central k-space segment and therefore reduce lipid bleed. The optimal weighting factor was determined experimentally. A further advantage of the addition of the first two echoes was the enhancement of

lactate signals. The overlapping area of segments *a* and *b* in *k*-space was treated identically as for the processing method 2 (see Fig. 2).

For all three processing methods, data were apodized with a radial cosine filter in the spatial domain (starting at 0.25 of maximum radius), zero-filled, and Fourier transformed. Minor signal losses due to imperfect refocusing pulses were estimated at 5% for each spin-echo. Its correction was done prior to the compensation for T_2 effects. After correction of B_0 shifts by referencing to the NAA peak-position (27), metabolite maps were created by spectral integration over 0.2 ppm (25). For the lipid images, spectral integration was performed over the same chemical shift range as that for lactate.

The nominal in-plane resolution (not counting the effects of spatial window functions and circular *k*-space) was 7.5 mm for Cho+Cre, NAA, and Lac images. Thus, the nominal voxel volume was 0.7 ml. However, we prefer to report the actual voxel volume based on the full width half maximum (FWHM) dimensions of the two-dimensional point-spread function (PSF) in which windows and circular *k*-space have been accounted for. The width of the PSF was 13 mm, and because the 2D-PSF profile has a circular symmetry, the actual voxel volume is 1.7 ml.

Protocol

The human subject protocol was approved by the intramural review board at the National Institutes of Health. Multi-spin-echo proton spectroscopic imaging studies were performed on normal human subjects ($n = 5$), and on a patient with a biopsy-proven high grade lymphoma (two separate studies). The measurement protocol was similar to the one previously described (25), and consisted of 1) gradient echo MRI to determine OVS coordinates; 2) RF transmitter gain adjustment and shimming; 3) adjustment of the CHESS pulse angle; 4) the MRSI measurement. Three slices were collected within a total *TR* of 3200 ms. Slice thickness was 13 mm, slice gap 7 mm. The echo signals were acquired during 128 ms using a spectral width of 2000 Hz. A 32 × 32 (circular) point *k*-space was sampled with a 24 × 24 cm field of view. The measurement time of the HSI experiment was 11 min. The total measurement time, including setup times, was 20 min.

RESULTS AND DISCUSSION

The processing method for lactate methyl signal (processing method 3) was first tested on phantoms. The lactate editing in the MSE-HSI method is based on the modulation of the methyl proton resonance in subsequent echoes due to the coupling with the methine proton. For optimal performance of the selection of the lactate doublet, the slice profile of the coupling methine proton should cover completely that of the methyl protons despite the difference of 2.9 ppm in chemical shift. As expected, phantom measurements (Fig. 3) showed a strong dependency of the slice profile for the methyl protons on the relative selection widths of the 90° and 180° RF pulses. An equal or smaller width for the 180° pulses led to distortion of the slice profile for the lactate methyl protons, and concomitant signal loss. A 10% larger selection width of the 180° pulses led to complete elimination of profile distortions. These measurements stress the importance of the choice of a slightly higher bandwidth for the 180° pulses as compared with the 90° pulse in the MSE-HSI sequence. The phantom measurements with the increased bandwidth of the 180° pulses showed good slice profiles for lactate methyl (Fig. 3a), even for the later echoes. Some additional signal loss (10–20%) was observed for every repeated echo over the

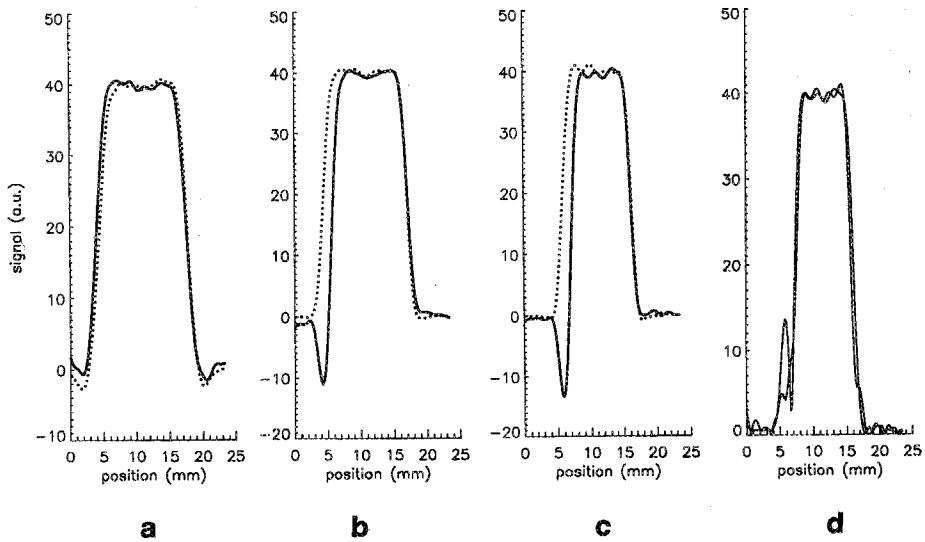

FIG. 3. Slice profiles of water and lactate, measured with a 2 *M* lactate phantom. (a)–(c) Profiles of water (dotted lines) and lactate (solid lines) in the first echo (real transverse magnetization). The lactate signal was inverted for comparison. By varying the slice selection gradient, the selection width of the 180° pulses was varied between +10%, equal, and −25% as compared with the selection width of the 90° pulse. The lower selection widths resulted in a deterioration of the lactate profile. (d) Lactate profiles of first and second echo are compared (magnitude transverse magnetization), using identical selection widths of 90° and 180° pulses. The second echo demonstrates a reduced amplitude of the side lobe, seen at the left of the profile.

full width of the profile, and could not be explained by T_2 effects. We tentatively attribute this loss to multiple quantum evolution during the refocusing pulses. Such an effect could increase if the RF bandwidth approaches the multiple quantum frequency.

Lipid distribution was tested in normal volunteers using processing method 1. As expected, lipid images showed only intensity above the noise level in the skull region due to incomplete lipid suppression with some "ringing" due to the limited number of phase encode steps. Note that the point-spread function for lipid is broadened with respect to that of the metabolites due the fact that a restricted *k*-space segment is used.

Overall, the measurements on normals demonstrated a spectral quality similar to that reported previously (25) with respect to water and lipid suppression. Processing method 2 for Cho+Cre, and NAA yielded a 10–25% improvement in image SNR as compared with the single echo multi-slice method (27) using *TE* 272 ms. The improved SNR is mainly due to the acquisition of the first echo at 136 ms. The NAA metabolite maps generally showed only minor bleed of lipid into brain regions similar to the single echo multi-slice method. In two volunteers, the top slices showed substantial lipid contamination. In these cases, improved NAA maps were obtained by discarding the signals from the first echo (SNR was traded off against lipid suppression).

To assess the viability of processing method 3 to register elevated lactate levels in human brain, a patient with high grade lymphoma was studied (Fig. 4-6). The lesion initiated within the right hemisphere (left in Fig. 5 and 6) and crossed the corpus callosum to penetrate the left hemisphere. No lipid presence could be demonstrated in the lesion using processing protocol 1. A spectrum from the center of the lesion in the left hemisphere (Fig. 4) showed elevated lactate and Cho+Cre, and reduced NAA. The reduced spectral resolution is the result of the limited acquisition time/echo (24). Metabolite maps were created of NAA, Cho+Cre, Cho/NAA, and lactate (Fig. 5). In the affected regions a marked increase of lactate and Cre+Cho was observed, whereas NAA was much reduced. A similar situation was observed in the follow-up study 2 months later.

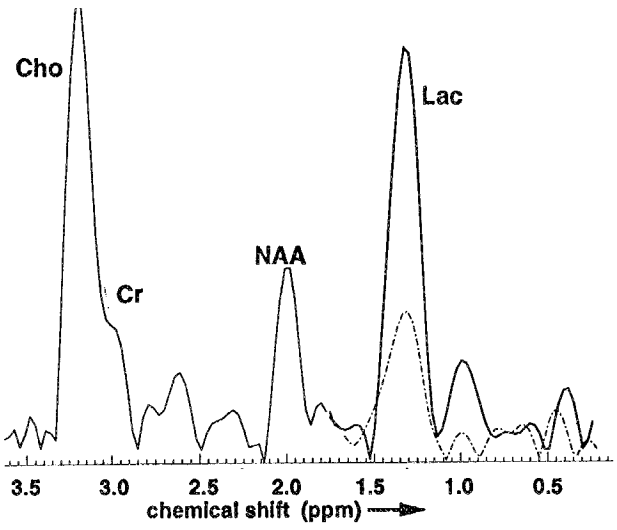

FIG. 4. Spectra from the lesion center acquired with multi-spin-echo proton MRSI method and processed with different methods. The low field (left) part of the spectrum was obtained with processing method 2 for noncoupled resonances. The high field (right) part was obtained with processing method 3 for lactate (solid line), and also with method 2 (dashed line). Note the increase in lactate signal using the lactate processing.

Data of the center slice of the latter study demonstrate the influence of different processing methods on the lactate and lipid maps (Fig. 6). The lipid image of Fig. 6b (processing method 1) shows high intensity in the skull region. When using only the second echo (at 272 ms), the lactate image should be similar to a conventional long echo-time spectroscopic imaging. Note the presence of some lactate intensity in the lesion and the high remaining lipid signals. The efficacy of the weighted subtraction of the first and second echo in the lactate images using protocol 3 is demonstrated by the large reduction in lipid signal in Figs. 6d–6f. These images also show the effect of including later echoes in the processing.

The presence of remaining lipid signal in the echo at 272 ms leads to the possibility of motion artifacts originating from the large lipid peaks in conventional proton spectroscopic imaging. In processing method 3 of the new technique, the lipid signal of the first and second echo are reduced drastically by the weighted subtraction. Because these echoes are only 136 ms separated in each scan, the procedure has a negligible sensitivity to motion of the head. This explains the observation that in all studies, remaining lipid signal in processing method 3 was much smaller than the images obtained with only the echo at 272 ms.

As can be seen from the strong remaining lipid signals at the skull region in Figs. 6d–6f, the three different processing methods for lipid, lactate methyl, and singlet methyl resonances do not represent 100% effective editing methods. In order to provide insight into the degree of selection, we have evaluated the point spread function for lactate and lipid using the different *k*-space analysis processing methods (Fig. 7). The T_2 of the compounds plays an important role in the degree of selection. At 1.5 T the T_2 of the resonances for lipid and the lactate methyl protons are about 85 (see ref. 28 and references therein), and 1200 ms, respectively (29). If processing method 1 (for resonances with short T_2) detects only a low lipid concentration around the lesion, we may safely neglect the residual lipid concentration in processing method 3 due to the weighted subtraction procedure. However, if substantial lipid accumulation is detected with processing method 1 the lactate image should be considered unreliable because subtraction errors in protocol 3 may be substantial due to uncertainty in lipid T_2 in the lesion. We have not yet detected lipid in brain lesions using the new method. However, we estimate that the threshold for discarding the reliable discrimination of lactate and lipid is when lipid signal in processing method 1 is significantly higher than the typical NAA intensity.

Lactate signal is eliminated completely in protocol 1 if the lactate methyl T_2 is 1 s, because of the weighting factor in processing method 3. Even for a decrease of the lactate T_2 to 600 ms, only 8% of the total lactate methyl signal will contribute to the "lipid" image. Thus, even

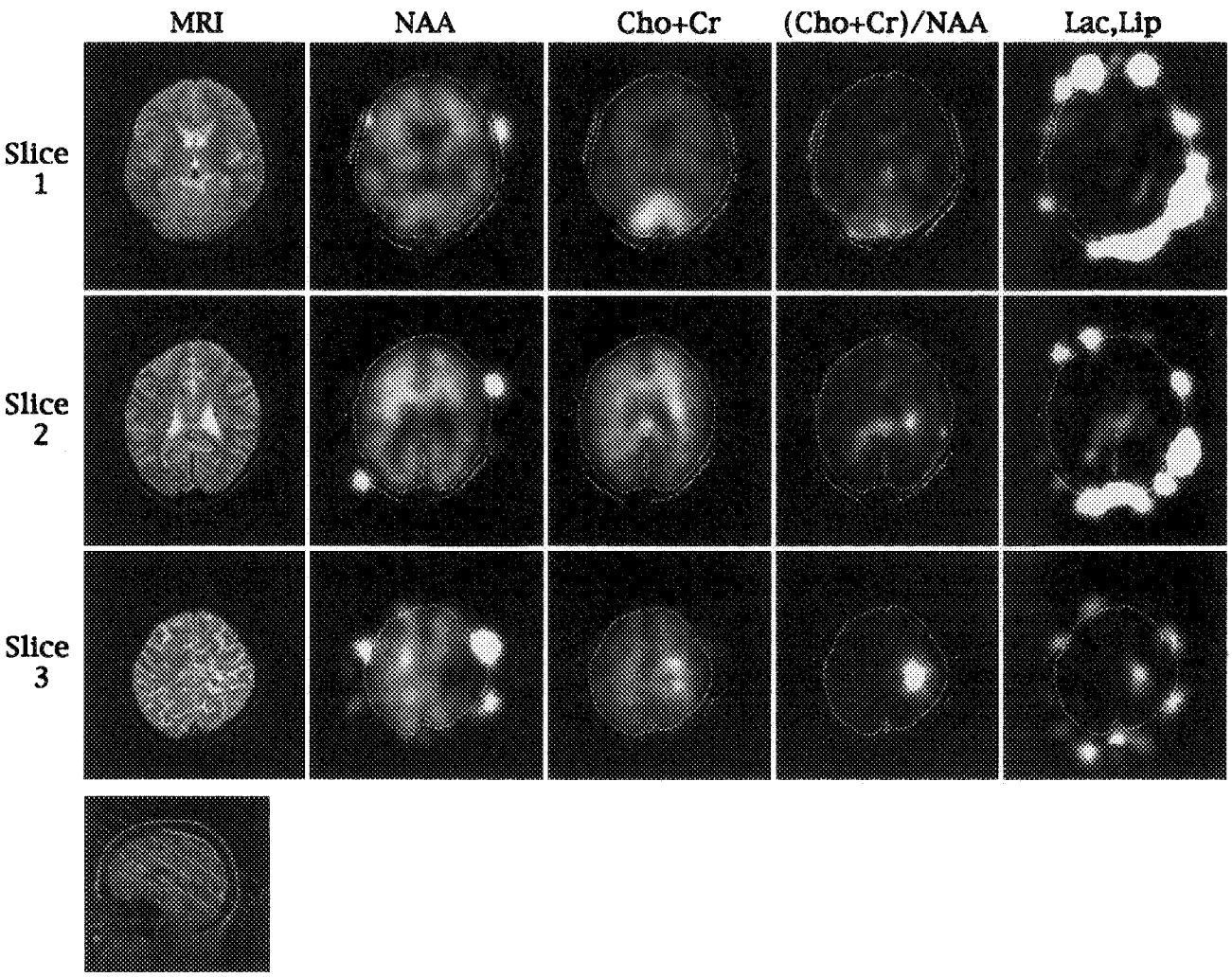

FIG. 5. Multi-spin-echo proton MRSI study of high grade lymphoma. The lymphoma initiated in the right hemisphere (left in images) posterior to the ventricles, and subsequently invaded the other hemisphere by crossing the corpus callosum. The affected regions show low NAA, high choline, and high lactate. The sagittal localizer image indicates the position of the three slices.

relatively large changes in lactate T_2 will not lead to substantial errors in the lactate/lipid discrimination.

On the other hand, changes in lipid T_2 could affect lipid/lactate discrimination. If the lipid image processing method does not show a significant intensity in or around the lesion, no significant lipid contribution to the lactate image is expected. If the lipid image processing method shows a distinct but low intensity at the lesion, then the weighting factor should be varied in the lactate processing method in order to minimize lipid contribution, and thus adjust for small lipid T_2 changes. Note that in the lymphoma cases reported in this paper, lipid was not detected in the lipid image processing method, and corrections in the lactate image were not necessary. For such a case with no lipid signal in the lesion, we estimate that the lower threshold for lactate detection in the new method is 1 m*M*. Note that lipid signals in the region of 1.3 ppm also contain homonuclear *J*-coupled resonances. Similar to the previous discussion, the short T_2 of these resonances would prevent the generation of artifacts in the lactate map.

It is useful to compare the new method with previous methods of proton MRSI. Let us start with a situation of lactate and lipid in a lesion with such relative concentration that at 272 ms *TE*, 50% of the peak intensity at 1.3 ppm originates from lactate and 50% from lipid. Simulating the resulting resonance shape may help, but is unsatisfactory because of nonideal shimming in the region, in particular when lipid is present. Possible solutions include the acquisition of images at *TE* 136 ms, or a double quantum filtered, "lactate edited" spectroscopic image (13). The latter takes 4 times the duration of the conventional MRSI (for similar SNR). Other editing procedures with higher SNR (e.g., ref. 8) may also become useful for MRSI. The first option gives unsatisfactory results because the image obtained at 136 ms will show an increased lipid contribution due to the short lipid T_2. Therefore, an additional method with different *TE* will not unambiguously detect the lactate contribution. In addition, conventional spectroscopic imaging at 136 and 272 ms will lead to large skull lipid signals, and are thus prone to motion artifacts. The proposed new method will not require any additional experiment time. However, the reliability of lipid/lactate separation depends on the lipid T_2.

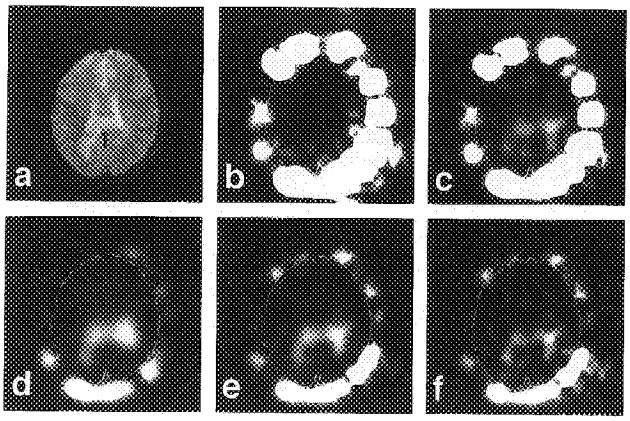

FIG. 6. Demonstration of the use of different processing methods on the same dataset. Data were obtained from a follow-up study of the high grade lymphoma patient (cf. Fig. 5). The location of the images is similar to that of slice no. 2 of Fig. 5. (a) Conventional gradient echo MRI. (b) Lipid image (processing method 1). (c) Lactate image obtained from the second echo (272 ms) only. (d) Lactate image using the first and second echo with the subtraction procedure of processing method 3. (e) Lactate image using the first, second, and third echo with the subtraction procedure of processing method 3 for the first two echoes. (f) Lactate image obtained with processing method 3 (all five echoes).

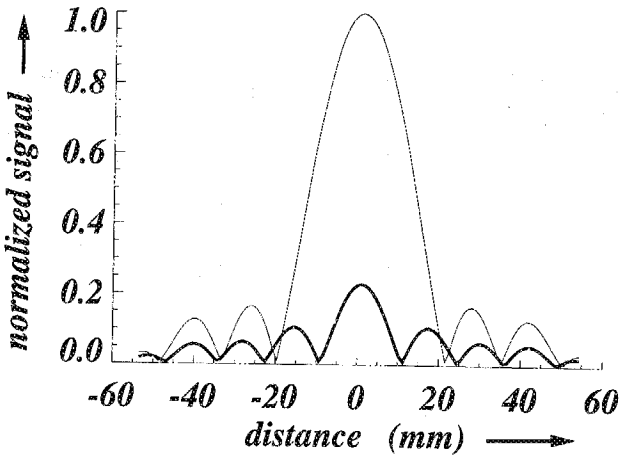

FIG. 7. The influence of the lactate processing protocol on the point spread function (PSF) of lipid signal. The thin line represents the lipid PSF in case the first echo is discarded (decay constant 110 ms). The thick line represents the lipid PSF following the subtraction procedure of the first and second echo (processing method 3). Note the large reduction in the central lobe and the significant suppression of side lobes.

This study demonstrated that different processing protocols, in combination with a particular *k*-space segmentation scheme and echo spacing, can be effectively used for fast proton spectroscopic imaging. Depending on the purpose of clinical studies, and the particular metabolite of interest, the methods may be modified to optimize the desired information density. For example, if lactate in stroke is the purpose of the study, the complete echo train could be extended such that the first echo is acquired at 272 ms. This will increase the quality of the lactate/lipid selection at the cost of the SNR of NAA, and Cho+Cre images. Due to the long T_2 of the lactate methyl protons, more echoes could be acquired to increase the speed of the method. Extensions to 3D proton spectroscopic imaging should be straightforward. The presented method can also be combined with a preceding inversion pulse for lipid suppression (30).

CONCLUSION

Improvements on a fast MRSI method have been presented allowing multi-slice metabolic imaging of lipid, NAA, Cho+Cre, and lactate within 11 min with a 1.7 ml voxel volume. The results demonstrate that a qualitative lipid/lactate discrimination can be obtained by different data processing methods. The quality of the lipid and lactate selection is high when the T_2 of both resonances does not differ significantly from the assumed values. In some cases, lactate evaluation in the presence of a large lipid concentration may be hampered by pathology specific lipid T_2 changes.

ACKNOWLEDGMENTS

The authors thank Peter van Gelderen for fruitful discussions, and Virginia Stark-Vancs for patient referral. The experiments were performed at the in vivo NMR research center, at the National Institutes of Health.

REFERENCES

1. D. L. Rothman, K. L. Behar, H. P. Hetherington, R. G. Shulman, Homonuclear ^{1}H double resonance difference spectroscopy of the rat brain *in vivo*. *Proc. Natl. Acad. Sci. (USA)* **81,** 6330–6334 (1984).
2. H. P. Hetherington, M. J. Avison, R. G. Shulman. ^{1}H homonuclear editing of rat brain using semi-selective pulses. *Proc. Natl. Acad. Sci. (USA)* **82,** 3115–3119 (1985).
3. S. R. Williams, D. G. Gadian, E. Proctor, A method for lactate detection *in vivo* by spectral editing without the need for double irradiation. *J. Magn. Reson.* **66,** 562–567 (1986).
4. E. Adalsteinsson, D. M. Spielman, G. A. Wright, J. M. Pauly, C. H. Meyer, A. Macovski, Incorporating lactate/lipid discrimination into a spectroscopic imaging sequence. *Magn. Reson. Med.* **30,** 124–130 (1993).
5. C. H. Sotak, A volume-localized, two-dimensional NMR method for the determination of lactate using zero-quantum coherence created in a stimulated echo pulse sequence. *Magn. Reson. Med.* **7,** 364–370 (1988).
6. D. M. Doddrell, I. M. Brereton, A selective excitation/B_0 gradient technique for high-resolution NMR studies of metabolites via zero-quantum coherence and polarization transfer. *NMR Biomed.* **2,** 39–43 (1989).
7. D. M. Doddrell, I. M. Brereton, L. N. Moxon, G. J. Galloway, The unequivocal determination of lactic acid using a one-dimensional zero-quantum coherence-transfer technique. *Magn. Reson. Med.* **9,** 132–138 (1989).
8. L. A. Trimble, J. F. Shen, A. H. Wilman, P. S. Allen, Lactate editing by means of selective-pulse filtering of both zero- and double-quantum coherence signals. *J. Magn. Reson.* **86,** 191–198 (1990).
9. J. E. van Dijk, A. F. Mehlkopf, W. M. M.J. Bovée, Comparison of in vivo zero and double quantum techniques. *NMR Biomed.* **5,** 75–86 (1992).
10. C. H. Sotak, D. M. Freeman, R. E. Hurd, The unequivocal determination of *in vivo* lactic acid using two-dimensional

double-quantum coherence-transfer spectroscopy. *J. Magn. Reson.* **78,** 355–361 (1988).
11. G. C. McKinnon, P. Boesiger, A one-shot lactate editing sequence for localized whole-body spectroscopy. *Magn. Reson. Med.* **8,** 355–361 (1988).
12. A. Knüttel, R. Kimmich, Double-quantum filtered volume-selectice NMR spectroscopy. *Magn. Reson. Med.* **10,** 404–410 (1989).
13. A. A. de Graaf, P. R. Luyten, J. A. den Hollander, W. Heindel, W. M. M.J. Bovée, Lactate imaging of the human brain at 1.5 T using a double-quantum filter. *Magn. Reson. Med.* **30,** 231–235 (1993).
14. R. E. Hurd, D. M. Freeman, Metabolite specific proton magnetic resonance imaging. *Proc. Natl. Acad. Sci. (USA)* **86,** 4402–4406 (1989).
15. M. von Kienlin, J. P. Albrand, B. Authier, P. Blondet, S. Lotito, M. Decorps, Spectral editing *in vivo* by homonuclear polarization transfer. *J. Magn. Reson.* **75,** 371–377 (1987).
16. D. Stryjewski, H. Oschkinat, D. Leibfritz, Detection of metabolites in body fluids and biological tissue by a 1D soft COSY technique. *Magn. Reson. Med.* **13,** 158–161 (1990).
17. C. L. Dumoulin, E. A. Williams, Suppression of uncoupled spins by single-quantum homonuclear polarization transfer. *J. Magn. Reson.* **66,** 86–92 (1986).
18. A. Knüttel, E. Rommel, M. Clausen, R. Kimmich, Integrated volume-selective/spectral editing ^{1}H NMR and postdetection signal processing for the sensitive determination of lactate. *Magn. Reson. Med.* **8,** 70–79 (1988).
19. A. Knüttel, R. Kimmich, Single-scan volume selective spectral editing by homonuclear polarization transfer. *Magn. Reson. Med.* **9,** 254–260 (1989).
20. I. M. Brereton, G. J. Galloway, S. E. Rose, D. M. Doddrell, Metabolite editing via correlated z order with total inherent coherence: ECZOTIC. *J. Magn. Reson.* **83,** 190–196 (1989).
21. I. M. Brereton, S. E. Rose, G. J. Galloway, L. N. Moxon, D. M. Doddrell, *In vivo* selective metobolite editing via correlated z-order. *Magn. Reson. Med.* **16,** 460–469 (1990).
22. R. Reddy, V. H. Subramanian, B. J. Clark, J. S. Leigh, Longitudinal spin-order-based pulse sequence for lactate editing. *Magn. Reson. Med.* **19,** 477–482 (1991).
23. D. Bourgeois, P. Kozlowski, A highly sensitive lactate editing technique for surface coil spectroscopic imaging in vivo. *Magn. Reson. Med.* **29,** 402–406 (1993).
24. J. H. Duyn, C. T. W. Moonen, Fast proton spectroscopic imaging of human brain using multiple spin-echoes, *in* "Proc., SMRM, 12th Annual Meeting, 1993," p. 316.
25. J. H. Duyn, C. T. W. Moonen, Fast proton spectroscopic imaging of human brain using multiple spin-echoes. *Magn. Reson. Med.* **30,** 409–414 (1993).
26. J. Slotboom, W. M. M.J. Bovee, The effect of bandwidth limited frequency selective pulses on the spin state of a weakly J-coupled spin system in the PRESS and SADLOVE localization sequences, *in* "Proc., SMRM, 12th Annual Meeting, 1993," p. 915.
27. J. H. Duyn, J. Gillen, G. Sobering, P. C. M. van Zijl, C. T. W. Moonen, Multisection proton MR spectroscopic imaging of the brain. *Radiology* **188,** 277–282 (1993).
28. E. M. Haacke, J. L. Patrick, G. W. Lenz, T. Parrish, The separation of water and lipid components in the presence of field inhomogeneities. *Rev. Magn. Reson. Med.* **1,** 123–154 (1986).
29. J. Frahm, H. Bruhn, M. L. Gyngell, K. D. Merboldt, W. Haenicke, R. Sauter, Localized proton NMR spectroscopy in different regions of the human brain in vivo. Relaxation times and concentrations of cerebral metabolites *Magn. Reson. Med.* **11,** 47–63 (1989).
30. D. Spielman, J. M. Pauly, A. Macovski, G. Glover, D. R. Enzmann, Lipid-suppressed single-and multisection proton spectroscopic imaging of the human brain. *J. Magn. Reson. Imaging* **2,** 253–262 (1992).